Mechanical Systems and Signal Processing ∎ (∎∎∎∎) ∎∎∎–∎∎∎

Contents lists available at ScienceDirect

Mechanical Systems and Signal Processing

journal homepage: www.elsevier.com/locate/ymssp

Acoustic emission source location in complex structures using full automatic delta T mapping technique

Safaa Kh. Al-Jumaili [a,b,*], Matthew R. Pearson [a], Karen M. Holford [a], Mark J. Eaton [a], Rhys Pullin [a]

[a] Cardiff School of Engineering, Cardiff University, Queen's Buildings, The Parade, Cardiff CF24 3AA, UK
[b] University of Basrah, Basrah, Iraq

ARTICLE INFO

Article history:
Received 18 September 2015
Received in revised form
10 November 2015
Accepted 19 November 2015

Keywords:
Acoustic emission
Source location
Complex structure
Unsupervised clustering
Delta T mapping technique

ABSTRACT

An easy to use, fast to apply, cost-effective, and very accurate non-destructive testing (NDT) technique for damage localisation in complex structures is key for the uptake of structural health monitoring systems (SHM). Acoustic emission (AE) is a viable technique that can be used for SHM and one of the most attractive features is the ability to locate AE sources. The time of arrival (TOA) technique is traditionally used to locate AE sources, and relies on the assumption of constant wave speed within the material and uninterrupted propagation path between the source and the sensor. In complex structural geometries and complex materials such as composites, this assumption is no longer valid. *Delta T mapping* was developed in Cardiff in order to overcome these limitations; this technique uses artificial sources on an area of interest to create training maps. These are used to locate subsequent AE sources. However operator expertise is required to select the best data from the training maps and to choose the correct parameter to locate the sources, which can be a time consuming process.

This paper presents a new and improved fully automatic delta T mapping technique where a clustering algorithm is used to automatically identify and select the highly correlated events at each grid point whilst the "Minimum Difference" approach is used to determine the source location. This removes the requirement for operator expertise, saving time and preventing human errors. A thorough assessment is conducted to evaluate the performance and the robustness of the new technique. In the initial test, the results showed excellent reduction in running time as well as improved accuracy of locating AE sources, as a result of the automatic selection of the training data. Furthermore, because the process is performed automatically, this is now a very simple and reliable technique due to the prevention of the potential source of error related to manual manipulation.

1. Introduction

Acoustic emission (AE) is a non-destructive testing (NDT) technique concerned with the passive monitoring of ultrasonic stress waves emitted from a variety of sources in a structure [1]. There are a variety of sources that cause AE which include

* Corresponding author at: Cardiff School of Engineering, Cardiff University, Queen's Buildings, The Parade, Cardiff CF24 3AA, UK. Tel.: +4402920877297,fax: +442920874939.
E-mail addresses: Al-JumailiSK@cardiff.ac.uk (S. Kh. Al-Jumaili), PearsonMR@cardiff.ac.uk (M.R. Pearson), Holford@cardiff.ac.uk (K.M. Holford), EatonM@cardiff.ac.uk (M.J. Eaton), PullinR@cardiff.ac.uk (R. Pullin).

http://dx.doi.org/10.1016/j.ymssp.2015.11.026
0888-3270/

crack propagation, friction, fretting and impact damage. These events will generate acoustic waves which can be detected at the structure's surface using piezoelectric transducers. The use of AE is important for SHM as it offers the potential for the real time monitoring of the health of a structure. The ability to track the early onset of damage and hence determine the structure's integrity will enable the switch from periodic inspections to a more condition based approach, therefore enabling increased inspection intervals, reducing structure downtime and maintenance costs. SHM techniques can be utilised to monitor hard to access structures such as off-shore wind turbines. One of the most attractive features of AE is the capability of source location and it is considered an important step for SHM [2]. For large-scale structures it is very costly and time consuming to inspect every part of the structure using the traditional techniques, such as X-ray and active ultrasonic techniques. If the damage location is known in advance it would enable maintenance teams to focus on particular areas of concern when using other NDE techniques. In addition, knowledge of the damage location can improve damage characterisation, because damage mechanisms are often dependent upon particular geometric features and loading conditions.

The conventional AE source location technique, known as the time-of-arrival or TOA technique, is discussed in detail in the NDT handbook [1]. It has been widely used to locate AE sources in isotropic and homogenous structures and is based on detecting the arrival time of an AE signal at each of the sensors for the fastest propagating mode, which enables the source to be located using a simple triangulation technique. The TOA technique relies on the assumptions of a constant wave speed in all directions from the source to sensor and an uninterrupted propagation path between the source and the sensor. In realistic structures the wave speed is rarely constant due to thickness changes and anisotropy in composite materials, where the wave velocity is dependent on the propagation direction, for instance the wave velocity of the fastest propagating mode is considerably higher in the fibre direction. Geometric features such as holes, lugs and structural discontinuities will also considerably affect the propagation path and velocity [3,4]. These factors mean that the assumptions relied upon by the TOA technique are not valid and hence will introduce errors in the source location calculation. In addition, any errors in the determination of signal arrival times will result in a further loss of accuracy in the estimated source locations. The threshold crossing approach, used commercially to pick the time of arrival of the AE signal is not satisfactory, because using a high threshold level will lead to inaccurate time of arrival measurement, while a lower threshold value will increase the ability to pick the accurate waveform onset but also increases the risk of a false trigger. In order to improve arrival time estimation a number of approaches have been investigated. The STA/LTA method compares the average energy in a short term window (STA) with the average energy in a long term window (LTA) prior to a point I in a signal [5]. The change in ratio indicates the signal arrival, however, despite good performance in noisy data the use of averages makes accurate determination difficult and a threshold is still needed to detect the change. The cross-correlation technique [6] has been used to find the arrival of a particular frequency within a signal by cross-correlation a short, single frequency, Gaussian windowed pulse with the recorded signal. An expansion of this is the use of wavelet transforms which identify energy arrival across a range of frequency. However it has been shown that the accuracy of this approach is poor in complex structures where multiple reflections are present [7]. Lokajicek and Klima [8] took the sixth order statistical moment of a sliding short time window which changes with the presence of structured data points associated to the signal. Although the moment is sensitive the detection of the change still relies upon a threshold. The use of neural networks has been investigated [9] however, its computational complexity limits its application in practice. A more reliable approach for arrival time estimation of seismic and ultrasonic signals adopts the Akiake information criteria (AIC) [10]. The AIC was first adapted for use directly on transient seismic data by Maeda [11]. However, more recently it has been demonstrated for accurate determination of arrival time of AE and ultrasonic transient signals [4,12–14]. The AIC function compares the signal entropy before and after each point i in a signal and returns a minimum at the signal onset where the greatest difference is seen between the high entropy random noise seen prior to signal onset and the low entropy structured signal after onset.

Attempts to improve upon the triangulation approach used in the TOA algorithm have been widely reported. AE source location in isotropic materials without prior knowledge of the wave speed has been reported by many researchers as an improvement over the simple TOA approach. These include the beamforming method [15,16] which is based on the delay-and-sum algorithm from small sensor arrays and the strain rosette technique [17] where the source location was predicted from the principal strain directions using rosette arranged macro-fibre composite (MFC) sensors. The modal acoustic emission method [18,19], where the AE wave modes in thin isotropic plates are predicted from the dispersion characteristics has also been used. The wavelet transform theory has been utilised to determine the arrival times of the different modes for one-dimensional [20] and two-dimensional location [7,21] respectively. AE location in anisotropic materials is challenging due to anisotropic propagation velocities. A number of interesting approaches have been taken to solving this problem [22–24] and improvements in accuracy have been shown in simple laminate plates. Ciampa et al. [25] utilised a specific layout of sensors to locate impact events in anisotropic materials without prior knowledge of the plate properties. Solution of a system of nonlinear equations is required in this technique. Kundu et al. [22] successfully developed a technique based on a cluster of sensors which was demonstrated in anisotropic plates and avoids the need to solve a system of nonlinear equations. Niri et al. [23] used the nonlinear Kalman Filtering algorithms (Extended Kalman Filter (EKF) and Unscented Kalman Filter (UKF)) as a probabilistic localisation algorithms to estimate the location of AE sources in anisotropic panels. Kundu et al. [24] present a two-step hybrid technique to locate sources in anisotropic plates. Wave propagation in a straight line is assumed in the first step to find the initial source location and solving an optimisation problem is the second step to improve the initial location accuracy.

Please cite this article as: S.Kh. Al-Jumaili, et al., Acoustic emission source location in complex structures using full automatic delta T mapping technique, Mech. Syst. Signal Process. (2015), http://dx.doi.org/10.1016/j.ymssp.2015.11.026

However none of these approaches account for structural complexities that may alter the wave propagation path and velocity, such as holes and thickness changes that may be present in reality. The development of the *Delta T Mapping (DTM) technique* accounts for these sources of error. The technique is a mapping approach whereby artificial sources are used to map a structure and thus allow high location accuracy on realistic complex structures. Originally developed for complex geometry metallic structures [26], the technique has also been shown to perform very well in anisotropic materials such as composites [27].

Although the DTM technique has shown the ability to locate with a high level of accuracy in complex structures, the collection and processing of training data can be very time consuming. It requires an operator with an AE background to select the optimal data to ensure the greatest possible accuracy. Furthermore, for locating AE sources a user must rely on experience and trial and error to determine processing parameters such as a suitable cluster diameter. Overcoming these problems will lead to a fully automatic process which would not relay on experience and would remove any human error whilst still maintaining or improving the accuracy of source location.

The objective of this paper is to extend the previous work on the DTM technique [26–29] and create a fully automatic technique which reduces human input and increases accuracy, reliability and the speed of the process.

The remainder of this paper is structured as follows: Section 2 will present the original *Delta T Mapping technique* in detail and describe the main limitations. The next section will present the main outline of the proposed methodology, followed by the experimental procedure for validation. The results are then presented and discussed and finally conclusions are drawn.

2. Original Delta-T Mapping technique methodology

According to Baxter [26] the main steps for the implementation of the DTM technique are outlined briefly below:

i. **Determine an area of interest and construct a grid system**: The DTM technique offers the ability for monitoring the complete structure or a part of it, which maybe of specific interest due to geometric features or known stress concentrations. A grid is constructed on the area of interest within which AE events will be located. A source which creates a broadband artificial AE source is preferable and different sensor types can be used to monitor the area of interest. Sensors can also be placed within the area of interest, as long as most of the sensors provide coverage with the area of interest within the sensor array.

ii. **Collect arrival time data from artificial sources at each grid node**: Hsu–Nielson (H–N) pencil lead fracture sources [30] are generated at each node position within the grid. The H–N source creates an artificial AE source which enables the determination of the TOA from source to sensors to be calculated for each sensor pair. Averaging the recorded TOAs of several events at each node of the grid is used to reduce source errors in the training data. Missing nodal data, as a result of holes, for example can be interpolated from the other surrounding nodes.

iii. **Calculate ΔT maps**: Once the TOA data for each node position has been collected the difference in arrival time (delta-T) for each sensor pair can be calculated, for example four sensors would results in six sensor pairs. Knowing the co-ordinates of each node results in the generation of average delta-T maps for each sensor pair. Contours of constant delta-T relative to all sensor pairs can be visualised as a resulting map.

iv. **Real AE data location**: Once real AE data has been collected, the delta-T for each sensor pair from a real AE event can be calculated. The resulting delta-Ts for each sensor pair can be represented by a line of constant delta-T which displays possible source locations. By overlaying these identified contours for each sensor pair a convergence point is identified, indicating the source location. As with the time of TOA technique, at least three sensors are required to provide a 2D source location. The confidence in source location estimation can be improved using additional sensors. Theoretically all lines should intersect at one location; however in reality, not all lines will cross at the same point. Therefore, to estimate the source location all convergence points are identified and a cluster analysis provides the most probable source location.

The traditional DTM technique used threshold crossing to determine the arrival times of the propagation waves at the sensors. The most recent version of DTM technique is known as the AIC DTM technique and was developed by [28,29] and overcame the limitation of arrival time calculation. Although the traditional DTM technique located successfully AE sources in different structural materials and complexity, the major disadvantage was the first threshold crossing approach which can generate erroneous locations when the actual signal onset is lower than the threshold level set. Pearson et al. [28,29] present a solution of this problem by exploiting the Akiake Information Criteria (AIC) [10] to determine the actual signal onset for both the training and the actual event data.

Although these iterations of the DTM approach have made improvements in location accuracy and reliability, there are still a number of limitations with this approach. Firstly, as mentioned above, several events are required to be generated at each node in the grid. Selection of the correct events and removing erroneous data is essential to constructing the training maps. Nominally this is conducted by recording times at which erroneous data occurred and by visual inspection by the operator, resulting in a lengthy process depending on the size of the grid. Secondly, only the convergence points inside a specific cluster diameter are used to calculate the probable AE source location (step 4). The optimum cluster diameter is

Please cite this article as: S.Kh. Al-Jumaili, et al., Acoustic emission source location in complex structures using full automatic delta T mapping technique, Mech. Syst. Signal Process. (2015), http://dx.doi.org/10.1016/j.ymssp.2015.11.026

determined by the operator by collecting data from known random node positions and comparing the error between actual and estimated source locations before testing commences. The optimum cluster diameter might not be same for all positions.

These limitations have a direct effect on the performance of the technique and result in less accurate probable source locations. The inclusion of incorrect events in each grid point will affect the training map accuracy and/or selecting non-optimum cluster diameters will affect source location accuracy. Furthermore, the process of manual selection of optimum training data is time consuming. This paper presents a new approach which overcomes these limitations.

3. Improved Delta T mapping technique

In order to reduce the sources of error related to the traditional DTM technique a fully automatic new DTM approach is presented here. This approach can be divided into two parts; firstly, selecting the valid events at each grid point using an unsupervised clustering technique and secondly, calculating the AE source location using the Minimum Difference approach [1,31], to eliminate any human manipulation of the data. The main new features of the fully automatic DTM technique are presented in the flowchart (Fig. 1). This section will describe each part of the new approach.

3.1. Selection of correct events

3.1.1. Unsupervised clustering methodology of AE events

After collection of the training data by applying artificial sources on each node position in the grid the time of arrival to each sensor is obtained. There is no restriction to the number of artificial sources used at each position, typically five to 10 H–N sources gives good repeatability. The classification process is applied at each grid position to select AE events which are highly similar to each other, where the input data vector for the clustering process is the time difference between sensors pairs and will be used for the similarity criteria.

In previous versions of the DTM technique, front end amplitude filters were used on the acquisition systems to remove erroneous data from additional hits arising from reflections from the specimen boundary. This ensured the number of hits in an event corresponded to the total number of used sensors. The front end filters required user experience to be set correctly and in larger structures often required changing during collection of the training data, both of which slowed the process. Erroneous data was still collected when a set of hits less than the number of used sensors and hits from bad pencil lead breaks were recorded respectively. These sources of erroneous data required manual removal by the user, again adding additional time to the process. However in this work, for each point of the Delta T grid, the recorded hits were separated automatically to create AE events using a time based approach. In this work all the used sensors were required to register a hit within a certain time window in order for it to be considered as an event. Simultaneously, the incorrect erroneous data

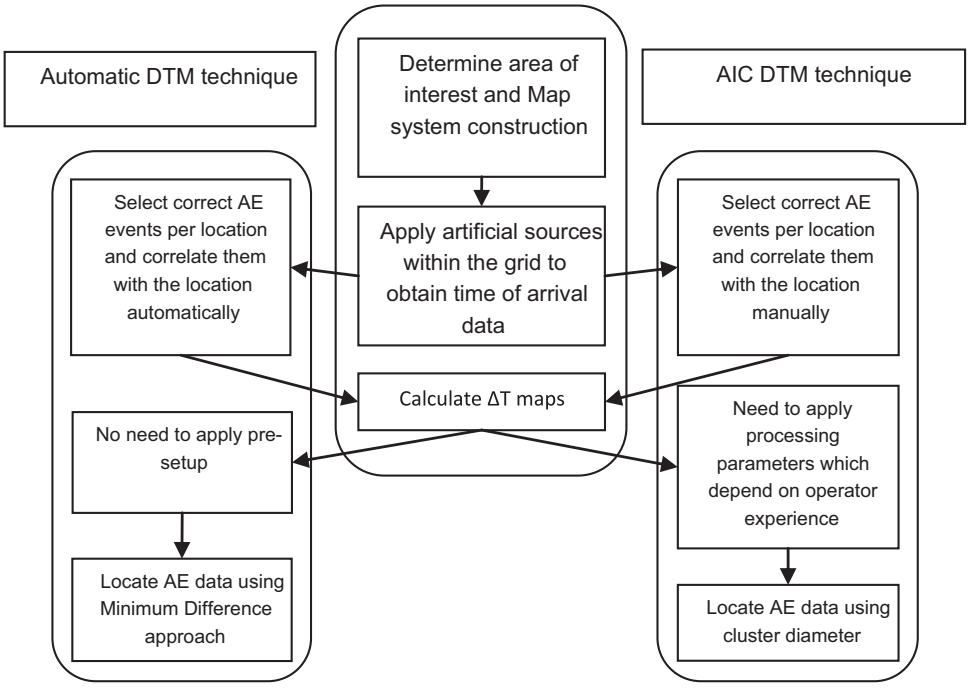

Fig. 1. Flow diagram representation of (a) automatic DTM technique and (b) AIC DTM technique.

Please cite this article as: S.Kh. Al-Jumaili, et al., Acoustic emission source location in complex structures using full automatic delta T mapping technique, Mech. Syst. Signal Process. (2015), http://dx.doi.org/10.1016/j.ymssp.2015.11.026

caused from those conditions mentioned above were automatically removed. Then, the AE hits from each point within the delta grid are correlated with the point coordinates (x, y) automatically, using time stamps placed by the operator within the collected data. Where the time stamps are placed in the data following acquisition from each grid node and are then used to automatically identify which hits are associated with each grid node.

3.1.2. Apply the unsupervised clustering

For each grid point within the map, in order to select the correct events to construct the training maps, an unsupervised classification is performed and the highly correlated events (similar to each other) are selected. The events are treated as pattern vectors and used as input to the unsupervised clustering. Each event is identified by the calculated difference in time of arrival for each sensor pair (e.g. the case of four sensors creates six sensor pairs 1–2, 1–3, 1–4, 2–3, 2–4 and 3–4). The correlation between events refers to the similarity between the events arrival time difference of their sensor pairs. A complete link hierarchical clustering algorithm [32] is then used to group events based on their similarity, or correlation coefficient.

The complete link hierarchical clustering algorithm for data of N events is described by the following steps:

i Assign each event to its own cluster (for N events we have N clusters).
ii Compute the distances (similarities) between clusters, where the distance is equal to the largest distance from any member of one cluster to any member of the other cluster.
iii Reduce the number of clusters by one through merging of the most similar pair of clusters.
iv Repeat steps 2 and 3 until all items are clustered into a single cluster.

At a higher level of correlation coefficient a greater number of groups will exist because the events in each group must be very highly correlated and vice versa, at a low correlation coefficient fewer groups will exist because each group can contain lesser correlated difference in time of arrival for each sensor pair. In this work the 0.99 correlation coefficient level from the largest group was selected and all events in this group were used (correlation coefficient of 1 means total correlation); each group at this level or above is deemed to contain highly correlated events and used for onward analysis. Conversely the groups are deemed to be suitably less correlated at a correlation level lower than the highest level. So, they are ignored and not used for onwards analysis.

3.1.3. Calculate ΔT maps

The average values of the difference in time of arrival for each sensor pair is calculated for the selected highly correlated events at each grid point. Finer resolution grids were created using interpolation between training data points in order to provide high precision of the location calculation results. In this work a 0.5 mm resolution was selected to perform the calculations.

3.2. Calculate location of real AE data

In order to overcome the need to identify the cluster size for calculation of the real AE data location, a new approach is presented here; this will be known as the Minimum Difference approach. This is a numerical approach, which is dependent on finding the point at which the difference between the source data and the training map data is minimised. There are four steps associated with the Minimum Difference approach which are described below:

i. Calculate source time difference: for each source using its sensors data, the arrival time difference of each sensor pair is calculated at that source. This step applies after the arrival time has been corrected using the AIC approach.
ii. Find the difference between the source pairs and the training maps pairs: Subtract each sensor pair time difference from the same sensor pair time difference of the training map.
iii. Sum the differences of all source sensors pairs (n) using Eq. (1):

$$sum = \sum_{1}^{n} |T\ source - T\ training\ map| \tag{1}$$

Where *T source* is the time difference of the source, *T training map* is the time difference of the training map.

iv. Find the point within the grid at which the minimum difference with the source time difference occurs. This point is taken to be the source position.

Using this approach will avoid any human interaction with the calculation process and therefore reduce the error source, increase result reliability and reduce the running time of the whole process.

A comparison between the conventional TOA, AIC Delta T mapping and new Automatic Delta T mapping for located AE events in a number of specimens will be presented in the experimental section of this chapter.

Please cite this article as: S.Kh. Al-Jumaili, et al., Acoustic emission source location in complex structures using full automatic delta T mapping technique, Mech. Syst. Signal Process. (2015), http://dx.doi.org/10.1016/j.ymssp.2015.11.026

4. Experimental procedure

In order to evaluate the performance of the improved DTM technique against the traditional TOA and the AIC DTM technique, two tests were conducted. The first was conducted on a simple geometry specimen made from 20 mm thick ASTM 516 gr 70 steel with overall dimensions of 90 mm × 2 m. At 17 mm from one end of the specimen a grid was constructed on the specimen with dimensions of 300 × 90 mm. Within this grid two geometric features were present; the first was 4.4 mm wide and 10 mm deep v-notch and the other was a 20 mm diameter half circle cut out as shown in Fig. 2. Six AE sensors were mounted to the specimen using silicone RTV adhesive (Loctite 595) to provide an acoustic coupling and a mechanical fixture (Fig. 2). Four MISTRAS Nano 30 sensors (sensors 1–4) and two MISTRAS WD sensors (sensors 5 and 6) were used and their relative positions are shown in Fig. 2. AE Data were recorded using a MISTRAS PCI-2 system with a 45 dB threshold and a 5 MHz sample rate. Prior to testing, Delta T Mapping training data was collected from the grid nodes at two resolutions, 10 mm resolution near the notch area (40 × 90 mm) and 20 mm resolution for the rest of the grid (Fig. 2). For the purpose of the training data 10 H–N sources were generated at each node on the grid. Ten arbitrary locations were selected within the grid and five H–N sources were performed at each position. The recorded signals, from all six sensors were used to calculate locations using the TOA, AIC DTM and the improved DTM. For the TOA technique an experimentally derived wave speed of 4600 m/s was used and the co-ordinates of the sensors were used as an input to the technique. The standard algorithm integrated in the AEwin software was used for the TOA location calculation. In practice, the standard approach involves the minimisation of the objective function X^2 in Eq. (2) [1], with respect to X_s and Y_s, the source position.

$$X^2 = \sum \left(\Delta t_{i,obs} - \Delta t_{i,calc}\right)^2 \tag{2}$$

where

$$\Delta t_{i,obs} = t_i - t_1$$

and

$$\Delta t_{i,calc} = \left[\sqrt{(X_i - X_s)^2 + (Y_i - Y_s)^2} - \sqrt{(X_1 - X_s)^2 + (Y_1 - Y_s)^2}\right] \times v^{-1}$$

t_1 and t_i are the arrival times at sensor 1 and the ith sensor in the array, v the wave speed in the given media, X_s, Y_s, X_1, Y_1, X_i and Y_i the x and y positions of the source, sensor 1 and the ith sensor respectively.

Furthermore, for the AIC DTM technique, visual inspection was used to remove erroneous events from each position in the training data grid.

To assess the performance of the improved DTM technique on a more complex geometry, a further test was conducted on an aerospace grade 2024-T3 aluminium plate, with dimensions of 370 × 200 mm with a thickness of 3.18 mm. The specimen contained a series of differing diameter circular holes as shown in Fig. 3. A MISTRAS PCI-2 system was used to record all AE data at 40 dB threshold and 2 MHz sampling rate. Four MISTRAS Nano-30s were adhered on the front face of the specimen (Fig. 3) using silicon RTV (Loctite 595). All transducers were connected to MISTRAS 0/2/4 pre-amps which had a frequency filter of 20 kHz to 1 MHz. The Delta T Mapping grid on the specimen covered an area of interest of 200 mm × 160 mm and had a resolution of 10 mm (Fig. 3). Five H–N sources were used at each node position within the grid. In order to assess the performance of the new Delta T mapping technique in a more complex structure, six arbitrary positions were selected within the Delta T grid and three H–N sources were conducted at each position. The average wave speed was calculated as 5400 m/s. Source locations were calculated using all four sensors for the three techniques.

Further investigation was conducted on the aluminium specimen using real AE sources. In order to generate AE from fatigue cracking a tension–tension fatigue test was conducted on the specimen until final failure. Load transfer was achieved using 20 mm loading pins with 5 mm steel plates connected either side of the specimen using seven M10 bolts at each end in order to distribute the load. The cyclic load regime was applied at 2 Hz in four batches. Initially a maximum load of 15 kN was applied for 7000 cycles followed by a maximum load of 20 kN for 18,000 cycles. Then the maximum load was increased to 22 kN and the test was run for 58,000 cycles. Finally the maximum load was increased to 24 kN and the test was run for 20,000 cycles before the final failure occurred. For the entire duration of the fatigue test the minimum load was fixed at 0.25 kN.

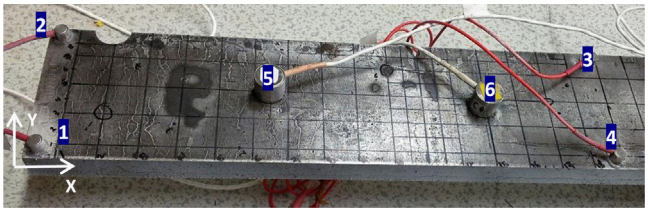

Fig. 2. Steel specimen configuration.

Please cite this article as: S.Kh. Al-Jumaili, et al., Acoustic emission source location in complex structures using full automatic delta T mapping technique, Mech. Syst. Signal Process. (2015), http://dx.doi.org/10.1016/j.ymssp.2015.11.026

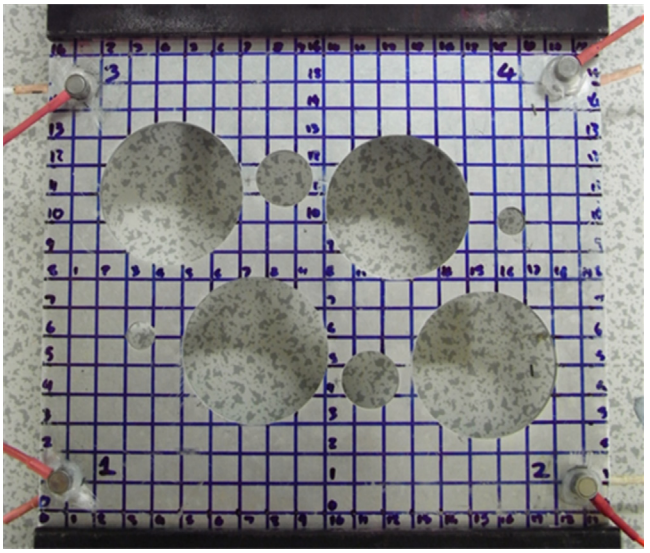

Fig. 3. Aluminium specimen configuration.

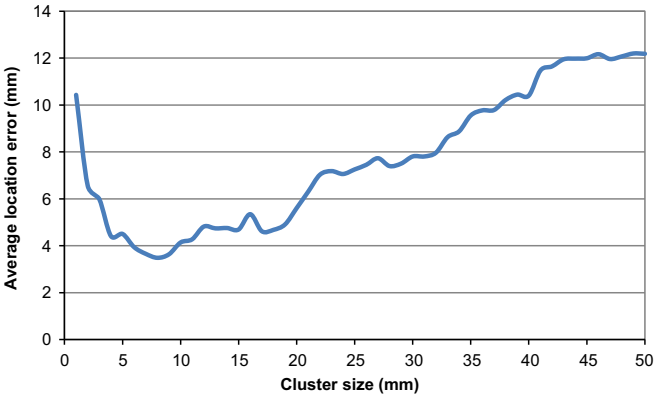

Fig. 4. Cluster size effect on the AIC Delta T accuracy.

5. Results and discussion

5.1. Validation testing on the simple steel specimen

For the AIC DTM location calculations, the optimal cluster size was calculated using a trial and error procedure, by assessing the accuracy of located AE events against the actual known positions. Fig. 4 shows the average location error (the Euclidian distance between the actual source position and the calculated source position) for the 50 sources versus the cluster diameter used in the AIC DTM algorithm. Basically, the optimal cluster size will refer to the lowest average error value and here in this work was selected to be 8 mm. But practically, the cluster diameter which gives the lowest average error for all source locations may not be the optimum diameter value for each source individually. Many source events will have the lowest location error at different cluster diameter values. As a result, choosing the optimum cluster diameter is a difficult process. It is clear that the cluster diameter has a significant effect on the location accuracy with the error ranging from less than 4 mm to over 12 mm depending on the diameter used. Selection the optimum cluster diameter is a time consuming process because it is nominally found using trial and error.

For the Automatic DTM source location calculations, the training maps are constructed by automatically removing the erroneous events for each grid positions using the unsupervised clustering procedure where only highly correlated events ($\geqslant$99%) are selected. The source locations are then calculated using the Minimum Difference approach. Finally, the TOA location results were exported directly from the MISTRAS AEwin software. The location results from H–N sources at 10 positions, calculated using the three location methods are presented in Fig. 5. It can be seen that there is marked improvement in source location accuracy using both of the DTM techniques over the traditional TOA technique due to the more accurate approach for the arrival time calculation. Furthermore, the Automatic DTM location accuracy slightly

Please cite this article as: S.Kh. Al-Jumaili, et al., Acoustic emission source location in complex structures using full automatic delta T mapping technique, Mech. Syst. Signal Process. (2015), http://dx.doi.org/10.1016/j.ymssp.2015.11.026

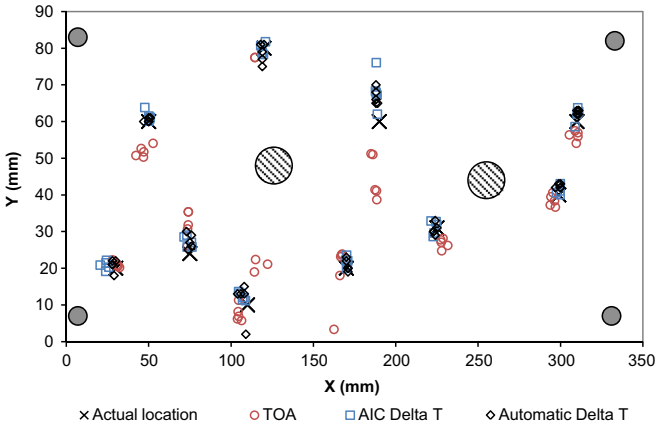

Fig. 5. Calculated source location by three techniques.

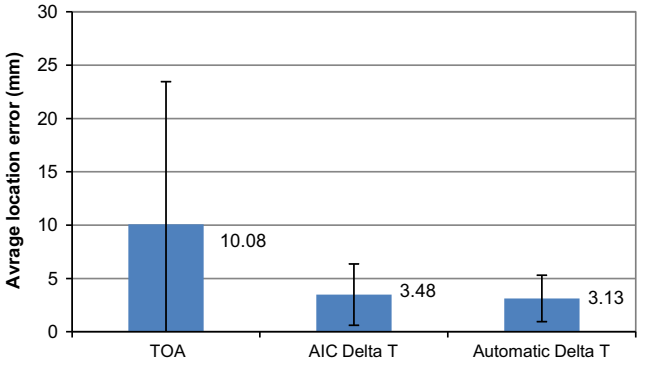

Fig. 6. Average location error for the three techniques result.

improves that of the AIC DTM due to using the new automatic selection of the correct events for constructing the training data and no longer requiring the use of the cluster diameter which prevents any human manipulation.

The average location error for the 50 sources, calculated as the Euclidian distance between the actual source position and the calculated source position, using the three location methods is presented in Fig. 6. The error bars in the figure represent one standard deviation above and below the average location error. It can be clearly seen that the average error is reduced significantly to 3.48 mm and 3.13 mm using the AIC and Automatic DTM techniques respectively compared with that of the TOA at 10.08 mm. These results are promising because the error is reduced to approximately 66% and 69% of the TOA error in this simple geometry, homogeneous specimen. Furthermore the Automatic DTM reduces the error by approximately 10% of the AIC DTM even though the process has been fully automatised and no longer requires an operator experience.

Further examination of the results reveals that the Automatic DTM not only improves the location accuracy but also speeds up the whole process and significantly reduces the time invested in implementing the technique. A comparison between the AIC and the Automatic DTM based on the time resources of the operator is provided in Table 1. From the table, the most time consuming step in the AIC DTM is represented by the selection and preparing of the AE data to construct the training maps, which was approximately 8 h for a small grid (similar to the one used in this work). On the other hand, the Automatic DTM is very fast and reduces the running time for constructing the training maps to approximately 18 s which is a significant improvement. Moreover, the new DTM does not require the trial and error process of determining the optimal cluster diameter when compared with the AIC DTM the cost is approximately 3.6 h.

These initial results are very promising findings, demonstrating the potential for the Automatic DTM technique to improve the location accuracy in comparison with the TOA and AIC DTM techniques. The automated technique is simpler to use, significantly reduces implementation time and simultaneously improves the reliability of location results.

5.2. Validation testing on the complex geometry aluminium specimen

The AIC DTM location calculations were determined using a 20 mm cluster diameter, which was concluded to be the optimum value using the trial and error procedure outlined earlier in this work. For the Automatic DTM location calculations the same procedure used for the steel specimen was implemented. Fig. 7 displays the located source from a series of H–N sources on the specimen for all three location techniques. The AIC and the Automatic DTM results show estimated sources

Please cite this article as: S.Kh. Al-Jumaili, et al., Acoustic emission source location in complex structures using full automatic delta T mapping technique, Mech. Syst. Signal Process. (2015), http://dx.doi.org/10.1016/j.ymssp.2015.11.026

Table 1
Running time comparison.

Stage	AIC Delta T (s)	Automatic Delta T (s)
Prepare the AE data to construct the training maps	about 28,800 (8 h)	18.19
Calculate the optimal Cluster size (try from 1 to 50 mm)	13,089	0
Calculate the source location	261.78	60.35
Total time	42,150.78	78.55

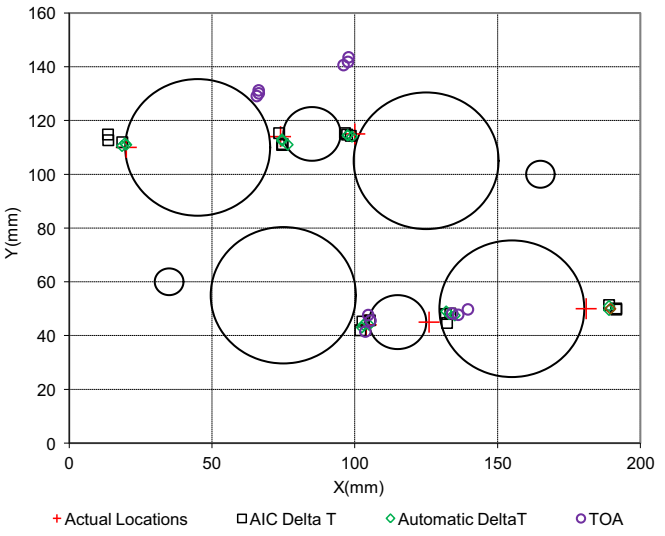

Fig. 7. Source locations on a complex specimen using three techniques.

very close to their actual location position. The TOA results show results distributed close to the actual position, far away from the position and outside the specimen boundary. This highlights the improved accuracy of both DTM techniques over traditional TOA approach to calculate source location in complex structure. The reasons for inaccurate results for the TOA technique are because the techniques relies on two assumptions, constant wave speed through the structure and a straight propagation line between the source and the sensor, both of which are difficult to achieve in real structures.

The average location error for all 18 sources (the Euclidian distance between the actual source position and the calculated source position) for all three techniques is presented in Fig. 8. The error bars represent plus and minus one standard deviation of the average. The average error of the DTM techniques is considerably lower than the TOA and offers an improvement in accuracy from 222 mm to approximately 5 mm. This figure presents two important points. Firstly, it highlights the fact that the TOA is not well suited to dealing with complex structures, as discussed previously. Secondly the new automatic DTM results show an improvement in accuracy over the AIC DTM results reducing the error from 4.96 mm to 3.88 mm

5.3. *Validation testing from fatigue testing*

The resulting fatigue crack after the specimen had been subjected to 96,000 fatigue cycles can be seen in Fig. 9. The location of the crack is in the high stress regions around the thin webbed section between the holes. The AE source location from the test was calculated using the three techniques, TOA and DTMs, using the same procedure as outlined earlier.

Due to the high quantity of recorded data from this test, the AE location results are presented in the form of spatially binned plots in order to ease representation of the data, these can be seen in Figs. 10–12. The area of interest was divided into 5×5 mm sub-sections with the cumulative events located in each bin presented in the figures. The location of the actual crack is highlighted by the red line in each figure. Fig. 10 shows the TOA source locations without any significant spatial bins with a high number of events. The highest sub-section contains about 20–60 events. This shows the inability of TOA to accurately locate AE sources in complex structures.

Fig. 11 and Fig. 12 show the AE source location calculations using the AIC and the Automatic DTM techniques, respectively. The figures show the significant area of events, 400 events for AIC DTM and 550 events of Automatic DTM, above the crack location. This area is located at around 15 mm from the location of the actual crack. These results show the high accuracy of the two mapping techniques in calculating the AE source location and significanctly lower resource requirement of the new technique.

Please cite this article as: S.Kh. Al-Jumaili, et al., Acoustic emission source location in complex structures using full automatic delta T mapping technique, Mech. Syst. Signal Process. (2015), http://dx.doi.org/10.1016/j.ymssp.2015.11.026

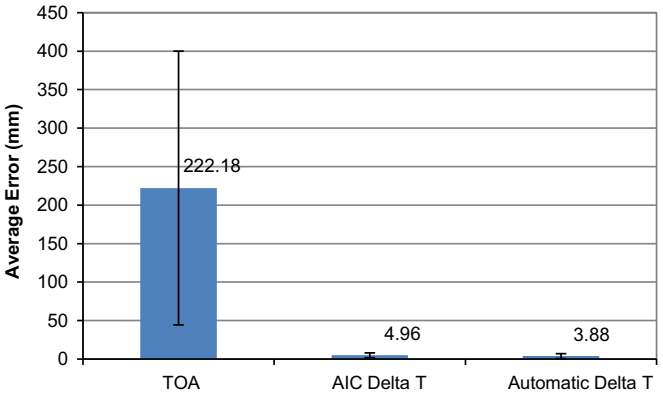

Fig. 8. Sources location error.

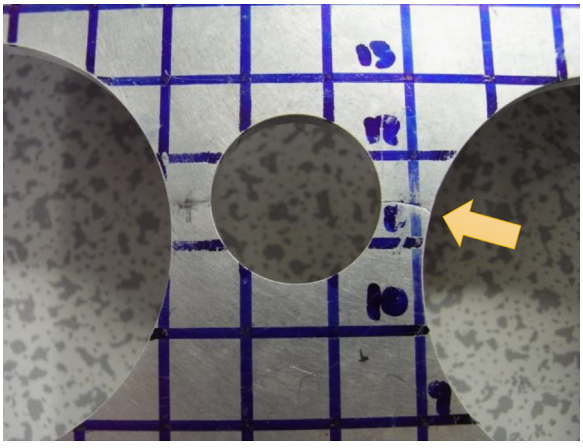

Fig. 9. Crack location after the final failure [28].

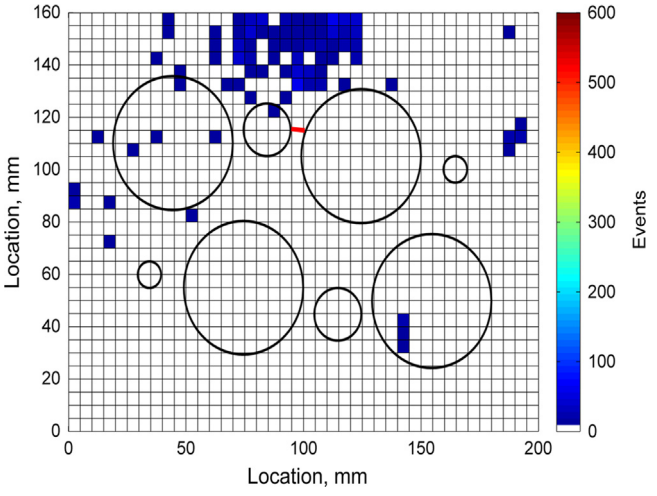

Fig. 10. TOA binned events locations. (For interpretation of the references to colour in this figure, the reader is referred to the web version of this article.)

Comparing the Automatic DTM with the TOA and the AIC DTM results highlights significant benefits such as the improvement in the accuracy and reliability of source location calculations. Experimental investigations on simple and complex structures have shown that the time consuming manual process has been replaced with a reliable automatic and less time consuming process which relies on a clustering algorithm.

Overall the new fullly Automatic DTM technique is a faster, easier to implement location technique which results in reducing testing downtime for set-up and requires less operator skill making it more compatible with commercial needs.

Please cite this article as: S.Kh. Al-Jumaili, et al., Acoustic emission source location in complex structures using full automatic delta T mapping technique, Mech. Syst. Signal Process. (2015), http://dx.doi.org/10.1016/j.ymssp.2015.11.026

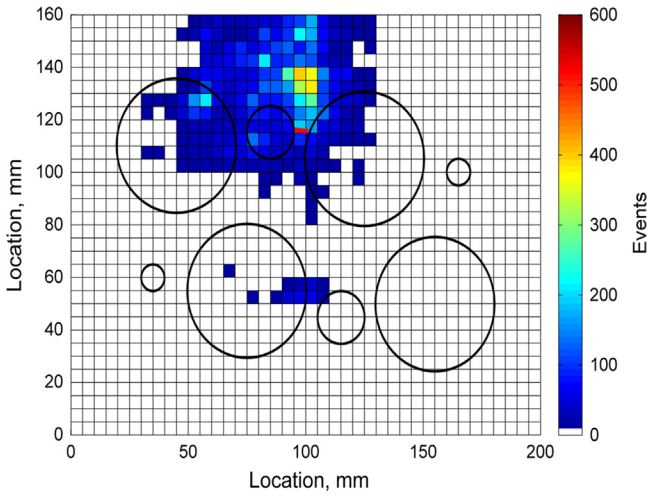

Fig. 11. AIC Delta T binned events locations. (For interpretation of the references to colour in this figure, the reader is referred to the web version of this article.)

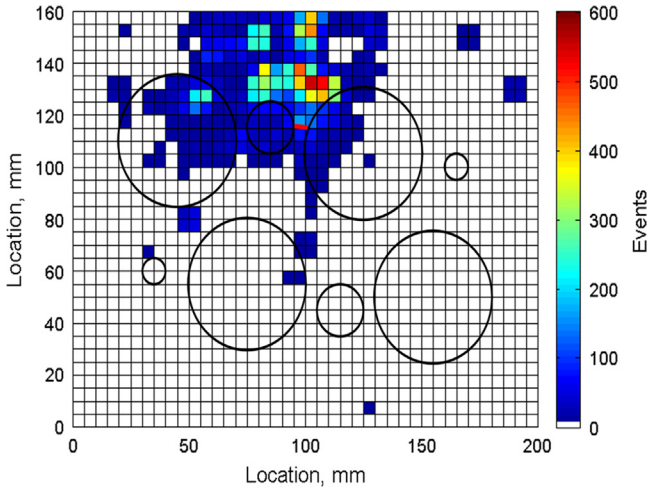

Fig. 12. Automatic Delta T binned events locations. (For interpretation of the references to colour in this figure, the reader is referred to the web version of this article.)

Having the automatic clustering technique for training data and the Minimum Difference approach for the AE source estimation reduces the potential for human error, the need for a skilled operators and manual process of selecting the optimal location cluster diameter.

6. Conclusions

A new fully Automatic DTM technique is introduced and verified experimentally using a variety of tests, in both simple and complex structures. The results obtained are excellent and demonstrate the success of the adopted methodology. The AIC DTM technique has been improved considerably as summarised below:

- Fast: The automatic selection and elimination of erroneous training data greatly decreases the process time from about 8 h to approximately 18 s.
- Increased reliability: Making the process fully automatic increases the reliability of the result and eliminates human error.
- Efficient: The process requires less resources in terms of time, operator skill and experience.
- More accurate: The technique was able to reproduce and even increase the accuracy of the already excellent accuracy of the AIC DTM technique, which was achieved in an automated and efficient way. It shows an increase in the accuracy for simple and complex geometry specimen. In simple geometry, the average location error is improved from 10 mm

Please cite this article as: S.Kh. Al-Jumaili, et al., Acoustic emission source location in complex structures using full automatic delta T mapping technique, Mech. Syst. Signal Process. (2015), http://dx.doi.org/10.1016/j.ymssp.2015.11.026

(using TOA) and (3.48 mm) (using AIC DTM) to only 3.13 mm. In complex structure, the average location error is improved from 222 mm (using TOA) and 4.96 mm (using AIC DTM) to only 3.88 mm using the Automatic DTM.

- Increased simplicity: No need for highly skilled operators to perform the process.
- More capability to apply in large scale structures.

The results of this study highlight the potential for the use of AE monitoring as a tool of SHM for damage localisation tasks; a high simplicity, fast, reliable, cheap and accurate technique has been presented. If this technique is integrated with commercial AE monitoring systems, it will be a powerful tool to provide real time highly accurate source location within complex large-scale components.

Acknowledgements

The authors would like to thank the Iraqi Ministry of Higher Education and Scientific Research for supporting this research and the technical staff of Cardiff University School of Engineering for their kind assistance with the testing programme.

References

[1] K.R. Miller, E.K. Hill, Non-Destructive Testing Handbook, Acoustic Emission Testing, American Society for Non-Destructive Testing, 2005.
[2] T. Kundu, Acoustic source localization, Ultrasonics 54 (2014) 25–38.
[3] R. Pullin, M. Baxter, M.J. Eaton, K.M. Holford, S.L. Evans, Novel acoustic emission source detection, J. Acoust. Emiss. 25 (2007) 215–223. ISSN 0730-0050.
[4] J. Hensman, R. Mills, S.G. Pierce, K. Worden, M. Eaton, Locating acoustic emission sources in complex structures using gaussian processes, Mech. Syst. Signal Process. 24 (2010) 211–223.
[5] P.S. Earle, P.M. Shearer, Characterization of global seismograms using an automatic-picking algorithm, Bull. Seism. Soc. Am. 84 (1994) 366–376.
[6] S.M. Ziola, M.R. Gorman, Source location in thin plates using cross-correlation, J. Acoust. Soc. Am. 90 (1991) 2551–2556.
[7] M. Hamstad, A. O'Gallagher, J. Gary, A wavelet transform applied to acoustic emission, J. Acoust. Emiss. 20 (2002) 39–61.
[8] T. Lokajíček, K. Klima, A first arrival identification system of acoustic emission (AE) signals by means of a high-order statistics approach, Meas. Sci. Technol. 17 (2006) 2461.
[9] J. Wang, T.-L. Teng, Artificial neural network-based seismic detector, Bull. Seism. Soc. Am. 85 (1995) 308–319.
[10] H. Akaike, Markovian representation of stochastic processes and its application to the analysis of autoregressive moving average processes, Ann. Inst. Stat. Math. 26 (1974) 363–387.
[11] N. Maeda, A method for reading and checking phase times in auto-processing system of seismic wave data, Zisin=Jishin 38 (1985) 365–379.
[12] J.H. Kurz, C.U. Grosse, H.-W. Reinhardt, Strategies for reliable automatic onset time picking of acoustic emissions and of ultrasound signals in concrete, Ultrasonics 43 (2005) 538–546.
[13] P. Sedlak, Y. Hirose, S.A. Khan, M. Enoki, J. Sikula, New automatic localization technique of acoustic emission signals in thin metal plates, Ultrasonics 49 (2009) 254–262.
[14] R. Sleeman, T. van Eck, Robust automatic P-phase picking: an on-line implementation in the analysis of broadband seismogram recordings, Phys. Earth Planet. Inter. 113 (1999) 265–275.
[15] T. He, Q. Pan, Y. Liu, X. Liu, D. Hu, Near-field beamforming analysis for acoustic emission source localization, Ultrasonics 52 (2012) 587–592.
[16] G.C. McLaskey, S.D. Glaser, C.U. Grosse, Beamforming array techniques for acoustic emission monitoring of large concrete structures, J. Sound. Vib. 329 (2010) 2384–2394.
[17] H.M. Matt, F.L. Di Scalea, Macro-fiber composite piezoelectric rosettes for acoustic source location in complex structures, Smart Mater. Struct. 16 (2007) 1489–1499.
[18] K.M. Holford, D. Carter, Acoustic emission source location, Key Eng. Mater. Trans. Tech. Publ. (1999) 162–171.
[19] H. Yamada, Y. Mizutani, H. Nishino, M. Takemoto, K. Ono, Lamb wave source location of impact on anisotropic plates, J. Acoust. Emiss. 18 (2000) 51.
[20] J. Jiao, C. He, B. Wu, R. Fei, X. Wang, Application of wavelet transform on modal acoustic emission source location in thin plates with one sensor, Int. J. Press. Vessel. Pip. 81 (2004) 427–431.
[21] N. Toyama, J.H. Koo, R. Oishi, M. Enoki, T. Kishi, Two-dimensional AE source location with two sensors in thin CFRP plates, J. Mater. Sci. Lett. 20 (2001) 1823–1825.
[22] T. Kundu, H. Nakatani, N. Takeda, Acoustic source localization in anisotropic plates, Ultrasonics 52 (2012) 740–746.
[23] E. Dehghan Niri, A. Farhidzadeh, S. Salamone, Nonlinear Kalman Filtering for acoustic emission source localization in anisotropic panels, Ultrasonics 54 (2014) 486–501.
[24] T. Kundu, X. Yang, H. Nakatani, N. Takeda, A two-step hybrid technique for accurately localizing acoustic source in anisotropic structures without knowing their material properties, Ultrasonics 56 (2015) 271–278.
[25] F. Ciampa, M. Meo, A new algorithm for acoustic emission localization and flexural group velocity determination in anisotropic structures, Compos. Part A: Appl. Sci. Manuf. 41 (2010) 1777–1786.
[26] M.G. Baxter, R. Pullin, K.M. Holford, S.L. Evans, T. Delta, Source location for acoustic emission, Mech. Syst. Signal Process. 21 (2007) 1512–1520.
[27] M.J. Eaton, R. Pullin, K.M. Holford, Acoustic emission source location in composite materials using Delta T mapping, Compos. Part A: Appl. Sci. Manuf. 43 (2012) 856–863.
[28] M. Pearson, Development of lightweight structural health monitoring systems for aerospace applications (Ph.D. thesis), Cardiff School of Engineering, Cardiff University, UK, 2013.
[29] M.R. Pearson, M. Eaton, C.A. Featherston, R. Pullin, K. Holford, Improved acoustic emission damage source location during fatigue testing of complex structures, in: Proceedings of the 34th Conference and the 28th Symposium of the International Committee on Aeronautical Fatigue and Structural Integrity (ICAF2015), Helsinki, Finland, 2015.
[30] N.N. Hsu, F.R. Breckenridge, Characterization and calibration of acoustic emission sensors, Mater. Eval. 39 (1981) 60–68.
[31] J.W. Scholey, P.D. Wisnom, M.R. Friswell, M.I. Pavier, M.J. Alika, MR, A generic technique for acoustic emission source location, J. Acoust. Emiss. 27 (2009) 291–298.
[32] A.M.R. Cluster, Analysis for Applications, Academic Press, New York, 1973.

Please cite this article as: S.Kh. Al-Jumaili, et al., Acoustic emission source location in complex structures using full automatic delta T mapping technique, Mech. Syst. Signal Process. (2015), http://dx.doi.org/10.1016/j.ymssp.2015.11.026